

---

# JOURNAL OF THE AMERICAN CHEMICAL SOCIETY

---

## Mo(OH)<sub>4</sub><sup>n+</sup> (n = 0, 2), Tetrahedral or Square-Planar? The d<sup>n</sup>-d<sup>10-n</sup> Hole Formalism for π-Donor and π-Acceptor Ligand Fields

R. H. Cayton, M. H. Chisholm,\* D. L. Clark, and C. E. Hammond

Contribution from the Department of Chemistry, Indiana University,  
Bloomington, Indiana 47405. Received January 29, 1988

**Abstract:** Fenske-Hall molecular orbital calculations have been used to probe the electronic structure and bonding of d<sup>0</sup> and d<sup>2</sup> monomeric transition metal tetraalkoxide complexes. A "frozen π-orbital" method was utilized to separate σ- and π-bonding effects of these ligands to the metal centers. Calculations on the model d<sup>2</sup> compound, Mo(OH)<sub>4</sub>, along the potential surface from a T<sub>d</sub> geometry to a square-planar D<sub>4h</sub> geometry, revealed a pronounced electronic preference for the D<sub>4h</sub> structure. This stabilization was found to be due to the generation of a metal-based nonbonding orbital, in the square-planar geometry, wherein the two metal electrons can reside. In the case of the model d<sup>0</sup> compound, Mo(OH)<sub>4</sub><sup>2+</sup>, the T<sub>d</sub> geometry was shown to be favored. The net (Mo|O) overlap populations and ligand orbital populations also indicate a square-planar d<sup>2</sup>, and a tetrahedral d<sup>0</sup> geometric preference. These results are consistent with the solid-state structures of W(OAr)<sub>4</sub> and Ti(OAr)<sub>4</sub>. A general electronic relationship was found to exist between high-valent and low-valent ML<sub>4</sub> complexes, and this phenomenon has been explained through the d<sup>n</sup>-d<sup>10-n</sup> hole formalism.

Organotransition metal chemistry has developed with soft, π-acceptor ligands such as carbonyl, nitrosyl, tertiary phosphines, and unsaturated hydrocarbons.<sup>1</sup> These ligands are well suited to coordinate to low-valent, electron-rich metal centers. The complementary nature of π-donor ligands (alkoxides, amides, thiolates) with electron-poor early transition elements in mid to high oxidation states is an aspect of organotransition metal chemistry of current interest. The capability of such ligands to act as π-donors is greatly dependent upon the metal d count and the corresponding availability of vacant d orbitals of appropriate symmetry to receive π-electrons.

Within the last several years there has been a renewed interest in the chemistry of mononuclear d<sup>0</sup>-d<sup>2</sup> compounds supported by homoleptic alkoxide and thiolato ligands.<sup>2</sup> A rather intriguing

class of these compounds is that which adheres to the general formula ML<sub>4</sub>, where M = a group IV or VI metal and L = an alkoxide or thiolate ligand. Although several such compounds have been successfully synthesized, only a few have been characterized by X-ray crystallography. These include Ti(OAr)<sub>4</sub>,<sup>3</sup> Mo(SBu')<sub>4</sub>,<sup>4</sup> W(SBu')<sub>4</sub>,<sup>5</sup> Mo(SAr)<sub>4</sub>,<sup>6</sup> and W(OAr)<sub>4</sub><sup>5</sup> (Ar = 2,6-C<sub>6</sub>H<sub>3</sub>-i-Pr<sub>2</sub>). Each of these species contains the metal in a +4 oxidation state; however, the group IV metals are formally d<sup>0</sup> whereas those of group VI are d<sup>2</sup>. Our interest in this system was further heightened by the structural differences exhibited through the series. For example, Ti(OAr)<sub>4</sub> is essentially tetrahedral with nearly linear Ti-O-C angles, Mo(SBu')<sub>4</sub> and W(SBu')<sub>4</sub> display

(3) Durfee, L. D.; Latesky, S. L.; Rothwell, I. P.; Huffman, J. C.; Folting, K. *Inorg. Chem.* **1985**, *24*, 4569.

(4) Otsuka, S.; Kamata, M.; Hirotsu, K.; Higuchi, T. *J. Am. Chem. Soc.* **1981**, *103*, 3011.

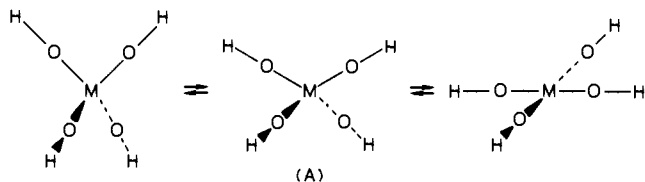
(5) (a) Listemann, M. L.; Dewan, J. C.; Schrock, R. R. *J. Am. Chem. Soc.* **1985**, *107*, 7207. (b) Listemann, M. L.; Schrock, R. R.; Dewan, J. C.; Kolodziej, R. M. *Inorg. Chem.* **1988**, *27*, 264.

(6) Roland, E.; Walborsky, E. C.; Schrock, R. R. *J. Am. Chem. Soc.* **1985**, *107*, 5795.

(1) Wilkinson, G.; Stone, F. G. A.; Abel, E. W., Eds. *Comprehensive Organometallic Chemistry*; Pergamon Press: New York, 1982.

(2) See, for example: Chisholm, M. H.; Rothwell, I. P. Alkoxides and Aryloxides. In Gillard, R. D.; McCleverty, J. A., Eds.; *Comprehensive Coordination Chemistry*; Pergamon Press: Oxford, 1988; p 335. Blower, P. J.; Dilworth, J. R. *Coord. Chem. Rev.* **1987**, *76*, 121.

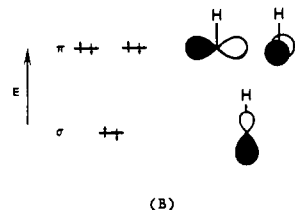
squashed tetrahedral cores, whereas  $\text{Mo}(\text{SAr})_4$  and  $\text{W}(\text{OAr})_4$  are nearly square planar. Because of these structural disparities we sought to investigate the electronic structure and bonding operative within this series, and to use these results to rationalize the geometric variations and physical properties observed for the system. The model system chosen was  $\text{Mo}(\text{OH})_4^{n+}$  ( $n = 0, 2$ ), wherein the geometry was varied from tetrahedral to square planar in a stepwise manner as shown in A. As a first approximation,



the Mo–O–H angles were constrained to be linear along the distortion coordinate. However, the effects of Mo–O–H angle variation were investigated for the extreme tetrahedral and square-planar geometries. Through the use of an overlap population analysis, and the Mulliken orbital populations, the observed structures can be readily understood. The Fenske–Hall molecular orbital method has been employed, the details of which are provided in the Appendix.

### Results and Discussion

We will begin with the derivation of the electronic structure of the model system  $\text{Mo}(\text{OH})_4$  in a tetrahedral geometry with Mo–O–H angles of  $180^\circ$ . The interaction of the alkoxide ligand with the molybdenum atom arises from the spatially and energetically inequivalent lone-pair orbitals of the free  $\text{OH}^-$  ligand, derived from an  $sp$ -hybridized oxygen atom. There is a relatively low-lying  $\sigma$  lone pair and a higher lying set of degenerate  $\pi$  lone pairs, depicted qualitatively in B. The set of four  $\text{OH}^-$   $\sigma$  lone-pair



orbitals transform as  $a_1 + t_2$  irreducible representations under  $T_d$  symmetry. Using the frozen  $\pi$ -orbital approximation (see Appendix),<sup>7</sup> interaction of the set of  $\sigma$  lone pairs with the molybdenum atom results in a splitting of the Mo 4d atomic orbitals into the expected  $e$  and  $t_2$  orbitals of a tetrahedron. The “ $\sigma$ -only” interaction is shown in the correlation diagram for  $T_d$   $\text{Mo}(\text{OH})_4$  in Figure 1. It can be seen in the center of Figure 1 that this procedure leaves the set of  $(\text{OH})_4^{4-}$   $\pi$  lone-pair orbitals unperturbed and allows for effective separation of  $\sigma$  and  $\pi$  interactions with the metal. Next we can “switch on” the  $\pi$  interaction and rationalize the effects on orbital energetics from simple perturbation theory. The set of eight  $\text{OH}^-$   $\pi$  lone pair orbitals transform as  $t_1 + t_2 + e$  irreducible representations in the  $T_d$  point group. The ligand  $t_1$   $\pi$  representation does not have the appropriate symmetry to interact with any metal d orbitals, and hence remains a pure O  $\pi$  lone-pair orbital in the  $T_d$   $\text{Mo}(\text{OH})_4$  molecule. Figure 1 shows that the  $\pi$  interaction with the  $(\text{OH})_4^{4-}$  ligand set of  $e$  symmetry is quite large, and this is easily rationalized in terms of a simple perturbation theory. The 2e “ $\sigma$ -only” metal orbital ( $d_{xz}, d_{xy}$ ) is the only metal orbital not destabilized by Mo–O  $\sigma$ -bonding. As a result, it is energetically the closest and has the best overlap with the  $\pi$  lone-pair orbitals. The resulting 1e orbital of  $T_d$   $\text{Mo}(\text{OH})_4$  is Mo–O  $\pi$ -bonding while the 2e orbital is its metal-based  $\pi$ -antibonding counterpart.

The  $t_2$  “ $\sigma$ -only” metal orbital ( $d_{xz}, d_{yz}, d_{x^2-y^2}$ ) also has a large overlap with the O  $\pi$  lone pairs, and interaction results in formation of the  $3t_2$  Mo–O  $\pi$ -bonding orbital. The perturbations imposed

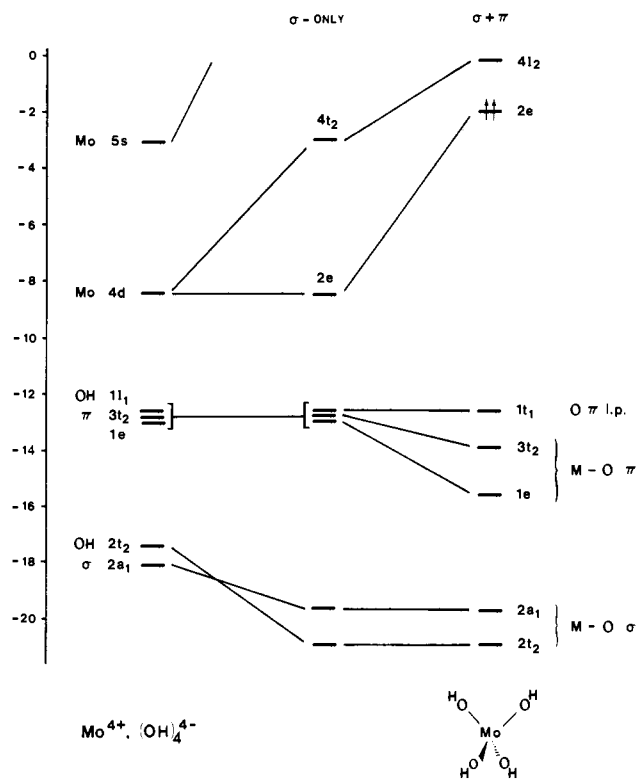


**Figure 1.** Frontier molecular orbital diagram for  $\text{Mo}(\text{OH})_4$  under  $T_d$  symmetry. The center column depicts the orbital energies resulting from the metal–ligand  $\sigma$  interactions, and the right side illustrates the combined metal–ligand  $\sigma + \pi$  interactions.

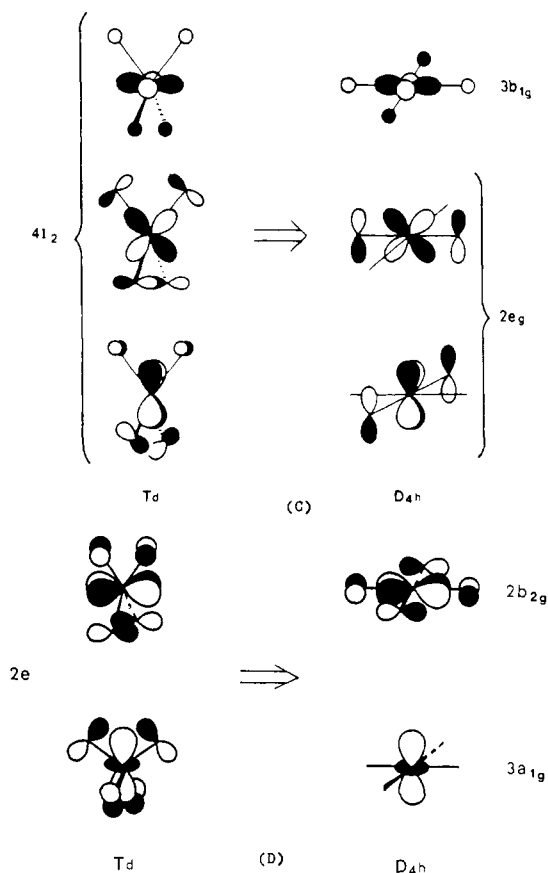
by the  $\pi$  interactions are denoted “ $\sigma + \pi$ ” (Figure 1) and demonstrate the relative magnitude of destabilization of  $e$  and  $t_2$  metal orbitals as a result of Mo–O  $\pi$ -bonding that occurs in low-lying orbitals of the same symmetry.

In  $\text{Mo}(\text{OH})_4$  the metal is in the (+4) oxidation state and formally  $d^2$ ; hence the HOMO of  $T_d$   $\text{Mo}(\text{OH})_4$  is the half-filled Mo-based 2e orbital. As was mentioned above, the Mo–O  $e$  interaction is the stronger of the  $\pi$  interactions. However, since the antibonding 2e orbital is half-occupied, the *net*  $\pi$ -bonding in the  $e$  set is diminished. This is evident in the small overlap population of 0.020 for the Mo–O  $e$  interaction as compared to 0.426 for the Mo–O  $t_2$   $\pi$  interaction. This appears to be the reason that the one structurally characterized group VI alkoxide,  $\text{W}(\text{OAr})_4$ , chooses to distort from a  $T_d$  geometry to nearly square planar.

### Tetrahedral–Square-Planar Distortion

In this section we will examine the electronic effects associated with distorting the tetrahedral  $\text{Mo}(\text{OH})_4$  molecule into a square-planar geometry. The variations in orbital energies for the primarily frontier orbitals of  $\text{Mo}(\text{OH})_4$  are depicted in the Walsh diagram in Figure 2. It should be noted that the Mo–O–H angles have been constrained to remain linear along the distortion coordinate. The effects of Mo–O–H bonding will be dealt with in a later section. The left side of Figure 2 portrays the frontier orbitals of  $\text{Mo}(\text{OH})_4$  in  $T_d$  symmetry which was derived earlier in Figure 1. As the tetrahedron is “flattened”, the symmetry is lowered to  $D_{2d}$  and eventually correlates to  $D_{4h}$  symmetry in the square-planar extreme. The Mo-based  $4t_2$  set (which is a combination of Mo–OH  $\sigma^*$  and  $\pi^*$  character in  $T_d$  geometry) is split markedly by the distortion as the  $x^2-y^2$  orbital becomes a pure Mo–OH  $\sigma^*$  interaction and is destabilized, while the  $xz$  and  $yz$  orbitals are slightly stabilized as they become pure Mo–OH  $\pi^*$  interactions. This effect is illustrated in C. The Mo-based 2e set of  $T_d$   $\text{Mo}(\text{OH})_4$  is also substantially split by the geometric isomerization. The  $xy$  orbital is destabilized by virtue of a stronger Mo–OH  $\pi^*$  interaction, while the  $z^2$  orbital is stabilized as it loses all of its Mo–OH  $\pi^*$  character and becomes the purely (98%) Mo-based nonbonding  $a_{2g}$  orbital, as illustrated in D.

(7) Roothaan, C. C. *J. Rev. Mod. Phys.* **1951**, *23*, 69.



The generation of a single metal-based nonbonding orbital appears to be an important stabilization force of the square-planar geometry for  $d^2$  complexes such as  $\text{W}(\text{OAr})_4$ . In the  $D_{4h}$  geometry, the two d electrons can be housed in a nonbonding orbital rather than in a  $\text{Mo}-\text{OH}$   $\pi^*$  orbital as dictated by the  $T_d$  geometry. This effect is reflected in the net  $\text{Mo}-\text{OH}$  overlap populations, shown in Figure 3, as they vary from the  $T_d$  to the  $D_{4h}$  geometry. The increase in total overlap population indicates a preferential  $\text{Mo}-\text{OH}$  bonding interaction in the square-planar ( $D_{4h}$ ) geometry for  $\text{Mo}(\text{OH})_4$ . The Mulliken populations (orbital occupancies) of the canonical orbitals of the  $(\text{OH})_4^{4-}$  ligand set also reflect this trend. Shown in Table I are the Mulliken populations of the  $(\text{OH})_4^{4-}$   $\sigma$  and  $\pi$  lone-pair orbitals before and after interaction with the metal center, in the various geometries along the distortion coordinate. The free ligand populations of the four  $\text{OH}^-$   $\sigma$  combinations and eight  $\text{OH}^-$   $\pi$  combinations are 8.00 and 16.00 electrons, respectively. After interaction, the decrease in population observed for the "coordinated ligand" is representative of the relative amount of electron density donated to the metal. The  $\sigma$  donation of the  $(\text{OH})_4^{4-}$  set does not vary appreciably with geometry; however, the  $\pi$  donation displays a substantial increase as the geometry approaches square planar.

The above results indicate that, electronically, group VI,  $d^2$ , tetraalkoxides prefer a square-planar ( $D_{4h}$ ) geometry over tetrahedral, providing that the steric bulk of the alkoxide ligands permits such a conformation. For example, the aryl ligands of  $\text{W}(\text{OAr})_4$  can arrange themselves in a "blade-like" manner such that the square-planar geometry is sterically feasible. On the other hand, the bulky alkoxide ligands of  $\text{Mo}(\text{O}i\text{Bu})_4$ ,  $\text{Mo}(\text{OCMeEt}_2)_4$ ,<sup>8</sup>  $\text{Mo}(\text{OC}t\text{Et}_3)_4$ ,<sup>8</sup> and  $\text{Mo}(\text{Oadamantyl})_4$ ,<sup>8</sup> apparently force the species to adopt a tetrahedral (or nearly so) conformation wherein the HOMO-LUMO gap is small, thus causing the compounds to be paramagnetic.

#### Geometric Preferences for the $d^0$ Case

Since the driving force toward the square-planar geometric preference in  $\text{Mo}(\text{OH})_4$  appeared to be the generation of a non-

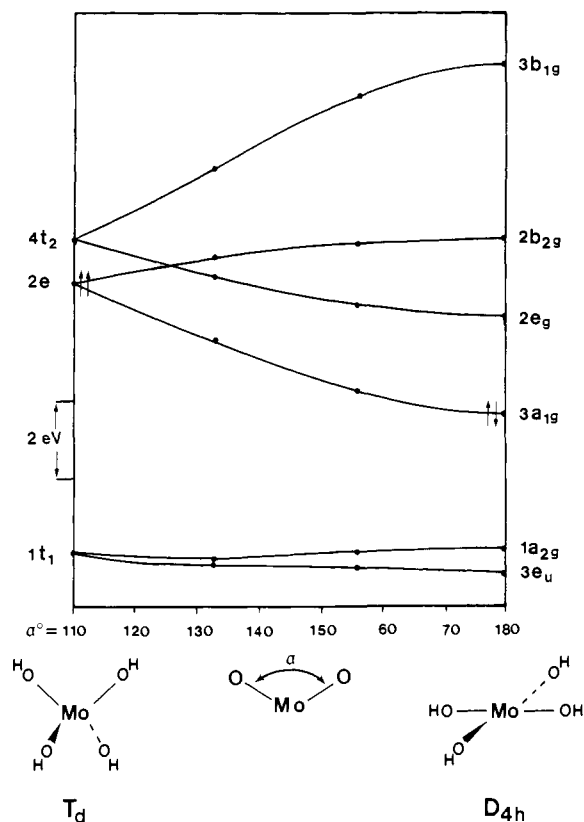


Figure 2. Walsh diagram for  $\text{Mo}(\text{OH})_4$  depicting the variations in orbital energies between the  $T_d$  and  $D_{4h}$  geometries. The angle  $\alpha$  is defined as the  $\text{O}-\text{Mo}-\text{O}$  angle between "trans"  $\text{OH}$  ligands.

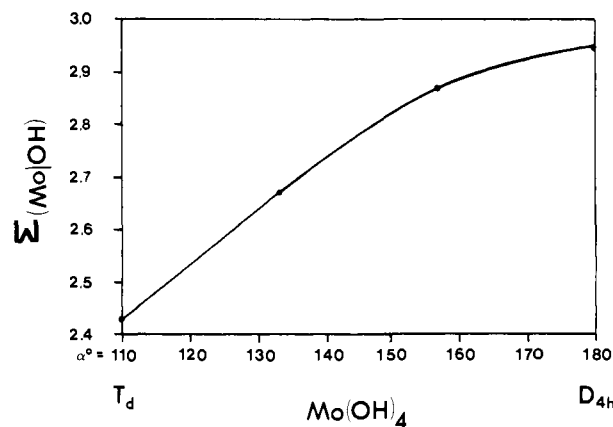


Figure 3. Variation in the total  $\text{Mo}-\text{OH}$  overlap populations of  $\text{Mo}(\text{OH})_4$  between the  $T_d$  and  $D_{4h}$  geometries.

Table I. Variation in the Mulliken Populations of the  $(\text{OH})_4^{4-}$   $\sigma$  and  $\pi$  Canonical Orbitals in  $\text{Mo}(\text{OH})_4$  from  $T_d$  to  $D_{4h}$  Geometry

	free ligand	O-Mo-O angle			
		110° ( $T_d$ )	133°	157°	180° ( $D_{4h}$ )
$\sigma$	8.0	6.51	6.62	6.58	6.61
$\pi$	16.00	14.58	14.47	14.28	14.18
$(\sigma + \pi)$	24.00	21.09	21.09	20.86	20.79

bonding metal-based orbital in which to house the two metal electrons, we felt it would be interesting to investigate the same potential surface for a  $d^0$  analogue. This was accomplished by the model system  $\text{Mo}(\text{OH})_4^{2+}$ . One such  $d^0$  species has been structurally characterized, namely,  $\text{Ti}(\text{OAr})_4$ . Although this compound boasts the same ligand set as  $\text{W}(\text{OAr})_4$ , in the  $d^0$  case the structure is nearly tetrahedral. Such a structural preference can be readily understood with the aid of the previously discussed Walsh diagram in Figure 2. Calculations on  $\text{Mo}(\text{OH})_4^{2+}$ , along

(8) Chisholm, M. H.; Hammond, C. E., unpublished results.

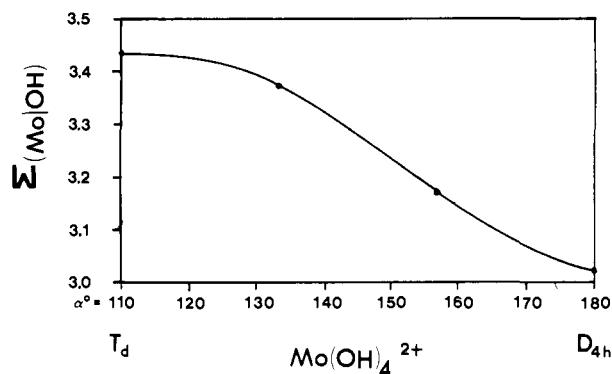


Figure 4. Variation in the total Mo-OH overlap populations of  $\text{Mo}(\text{OH})_4^{2+}$  between the  $T_d$  and  $D_{4h}$  geometries.

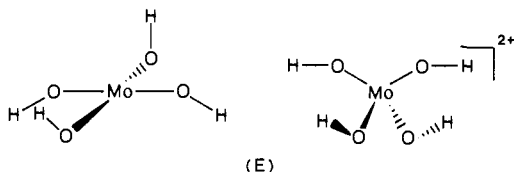
Table II. Variation in the Mulliken Populations of the  $(\text{OH})_4^{4-}$   $\sigma$  and  $\pi$  Canonical Orbitals in  $\text{Mo}(\text{OH})_4^{2+}$  from  $T_d$  to  $D_{4h}$  Geometry

	free ligand	O-Mo-O Angle			
		110° ( $T_d$ )	133°	157°	180° ( $D_{4h}$ )
$\sigma$	8.00	6.36	6.39	6.46	6.46
$\pi$	16.00	13.38	13.41	13.41	13.54
$(\sigma + \pi)$	24.00	19.74	19.80	19.87	20.00

the same distortion coordinate as shown in Figure 2, yield analogous orbital energy variations, the only difference being that the HOMO of  $\text{Mo}(\text{OH})_4^{2+}$  is the highest energy ligand lone-pair orbital ( $1t_1$  for  $T_d$ ,  $1a_{2g}$  for  $D_{4h}$ ). Since no metal-based orbitals are occupied, the  $T_d$  geometry provides the most stable metal-ligand bonding interactions. The preference for a  $T_d$  ligand environment is further reinforced by the net overlap populations of the metal-ligand interactions. These are depicted in Figure 4 for  $\text{Mo}(\text{OH})_4^{2+}$  as the geometry is varied from  $T_d$  to  $D_{4h}$ . The trend is exactly opposite that of  $\text{Mo}(\text{OH})_4$  (Figure 3), and the  $T_d$  conformation is clearly favored. In comparing the two curves, one interesting point emerges. The total Mo-OH overlap population for  $\text{Mo}(\text{OH})_4$  in the  $D_{4h}$  geometry (Figure 3) is nearly identical with that of  $\text{Mo}(\text{OH})_4^{2+}$  in the same geometry (Figure 4) ( $\text{Mo}(\text{OH})_4$ , 2.92;  $\text{Mo}(\text{OH})_4^{2+}$ , 3.02). In other words, in the square-planar geometry, occupation, or deoccupation of the  $3a_{1g}$  orbital has only a very slight effect on the net metal-ligand bonding. Such an effect would be expected based on the essentially nonbonding nature of the  $3a_{1g}$  orbital.

### Mo-O-H Bending

In the crystal structure of  $\text{Ti}(\text{OAr})_4$  the Ti-O-C angles average  $166^\circ$ . Likewise, the solid-state structure of  $\text{W}(\text{OAr})_4$  exhibits W-O-C angles averaging  $156.5^\circ$ . Although these angles deviate only slightly from linearity, we felt it important to investigate such an effect on the bonding in our model systems. Using the model compound,  $\text{Mo}(\text{OH})_4$ , the Mo-O-H angles were varied from  $180$  to  $133^\circ$ , while constraining the  $\text{Mo}(\text{O})_4$  core to remain square planar. The H atoms were rotated in a plane perpendicular to the  $\text{Mo}(\text{O})_4$  plane so as to mimic the structure of  $\text{W}(\text{OAr})_4$ . In the case of the  $\text{Mo}(\text{OH})_4^{2+}$  model system, the Mo-O-H angles were again varied from  $180$  to  $133^\circ$ , but the  $\text{Mo}(\text{O})_4$  core was kept tetrahedral. The H atoms were rotated in two mutually perpendicular planes in order to model the angular derivations in  $\text{Ti}(\text{OAr})_4$ . The representative models are illustrated in E. The



net Mo-O overlap populations representing the interactions between the  $(\text{OH})_4^{4-}$  ligand set and the metal center for both the  $\text{Mo}(\text{OH})_4$  and  $\text{Mo}(\text{OH})_4^{2+}$  model systems are shown in Figures 5 and 6, respectively. In both cases, deviation from linear Mo-

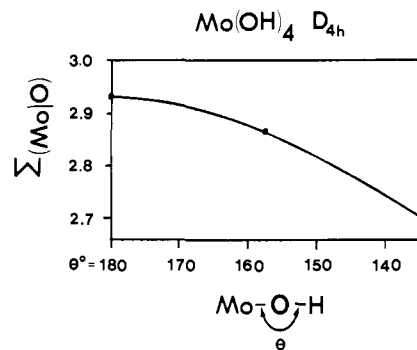


Figure 5. Variation in the total Mo-OH overlap populations of  $\text{Mo}(\text{OH})_4$  in the  $D_{4h}$  geometry as the Mo-O-H angles are varied from linear to  $133^\circ$ .

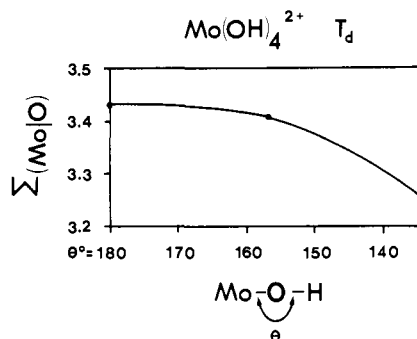


Figure 6. Variation in the total Mo-OH overlap populations of  $\text{Mo}(\text{OH})_4^{2+}$  in the  $T_d$  geometry as the Mo-O-H angles are varied from linear to  $133^\circ$ .

O-H angles causes a decrease in metal-ligand bonding. Hence, it would appear that the Mo-O-C bending in the solid-state structures of  $\text{W}(\text{OAr})_4$  and  $\text{Ti}(\text{OAr})_4$  is likely a result of steric rather than electronic factors. Of course, our model ligand set does not account for the aromatic  $\pi$ -system associated with the Ar ligands which may exhibit a subtle electronic effect on the conformational preferences of  $\text{W}(\text{OAr})_4$  and  $\text{Ti}(\text{OAr})_4$ .

### $d^n-d^{10-n}$ Hole Formalism

Now that the electronic structure and bonding in the square-planar  $\text{Mo}(\text{OH})_4$  and tetrahedral  $\text{Mo}(\text{OH})_4^{2+}$  model compounds have been addressed, we note some rather fascinating similarities and differences between these high-valent, early transition metal systems containing  $\pi$ -donor ligands, and the now "classical" low-valent, late transition metal systems containing  $\pi$ -acceptor ligands. For example, the square-planar structure of high-valent,  $d^2$ ,  $\text{W}(\text{OAr})_4$  is analogous to that exhibited by low-valent,  $d^8$ ,  $\text{ML}_4$  complexes such as  $\text{Pt}(\text{CN})_4^{2-}$ . Likewise, the high-valent,  $d^0$ , compound  $\text{Ti}(\text{OAr})_4$  adopts the same tetrahedral structure as low-valent,  $d^{10}$ , systems such as  $\text{Ni}(\text{CO})_4$ . This analogy may be described as a  $d^n-d^{10-n}$  hole formalism. That this analogy is electronic in origin can be illustrated by examining the square-planar  $d^2-d^8$  relationship. Let us first perform some simple electron counting for the square-planar  $\text{Mo}(\text{OH})_4$  molecule. Under  $D_{4h}$  symmetry, the  $(\text{OH})_4^{4-}$  ligand set donates four electron pairs to  $\sigma$ -bonding ( $a_{1g} + b_{1g} + e_u$ ) and three electron pairs to  $\pi$ -bonding ( $b_{2g} + e_g$ ). Thus, for electron counting, we have eight  $\sigma$  electrons, six  $\pi$  electrons, and two metal d electrons for a total valence count of 16. It is no accident that this is the same electron count observed for "classical"  $d^8$  square-planar complexes with  $\pi$ -acid ligands. Let us consider the following square-planar  $\text{ML}_4$  model. Under  $D_{4h}$  symmetry the four metal-ligand  $\sigma$  bonds transform as  $a_{1g} + b_{1g} + e_u$ , and thus the metal s ( $a_{1g}$ ),  $d_{x^2-y^2}$  ( $b_{1g}$ ), and  $p_x/p_y$  ( $e_u$ ) atomic orbitals can be used to form the four metal-ligand  $\sigma$  bonds. This will be true for both  $\pi$ -donor and  $\pi$ -acceptor ligands since it is a " $\sigma$ -only" interaction. The metal d orbitals which remain are the  $d_{z^2}$  ( $a_{1g}$ ),  $d_{xy}$  ( $b_{2g}$ ), and  $d_{xz}/d_{yz}$  ( $e_g$ ) atomic orbitals and these are shown in the center column of the correlation diagram in Figure 7. If the ligand set has orbitals

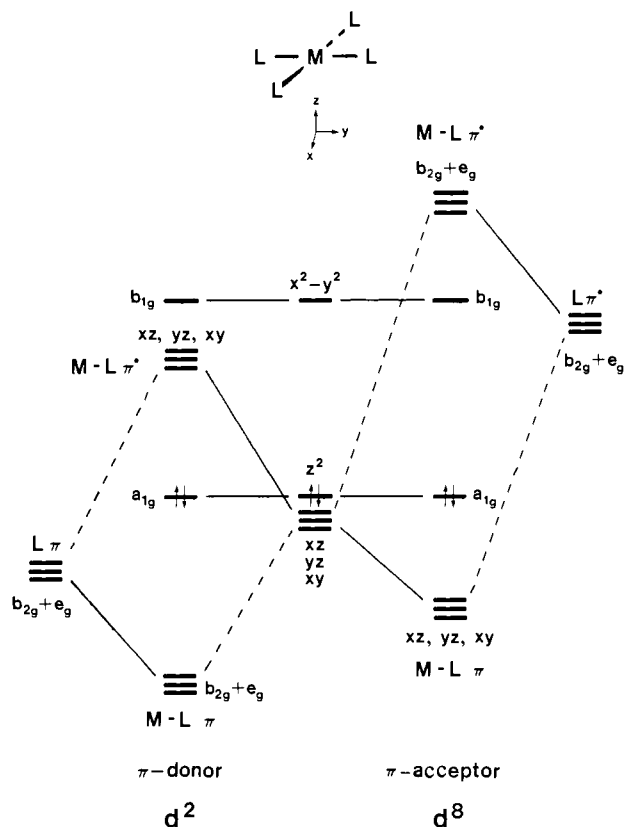


Figure 7. Qualitative correlation diagram for square-planar  $\text{ML}_4$  complexes illustrating the  $d^2$ - $d^8$  relationship between high-valent complexes with  $\pi$ -donor ligands (left) and low-valent complexes with  $\pi$ -acceptor ligands (right).

of  $\pi$  symmetry, then there are symmetry matches for the  $b_{2g}$  and  $e_g$  orbitals. This allows for the formation of three  $\pi$  bonds as seen for  $\text{Mo}(\text{OH})_4$ . If the ligands are  $\pi$ -acceptors, then  $\pi$  back-bonding from occupied metal  $b_{2g}$  and  $e_g$  orbitals into the vacant  $\pi$ -acceptor orbitals will stabilize the metal  $b_{2g} + e_g$  combination, leaving a stable electron count for a  $d^8$  metal center with a total of 16 valence electrons. This is shown on the right of Figure 7. By contrast, if the ligands are  $\pi$ -donors as in alkoxides, then ligand  $\pi$ -donation into the same set of metal  $b_{2g} + e_g$  orbitals will destabilize them leaving a stable electron count for a  $d^2$  metal center with a total of 16 valence electrons. This is shown schematically on the left of Figure 7, and forms the basis of our  $d^2$ - $d^8$  "hole formalism" for 16-electron square-planar compounds. For the early transition

metal center with  $\pi$ -donor ligands there is an overall arrangement of one low-lying occupied metal orbital with four high-lying virtual metal orbitals as shown in Figure 7. For the late transition metal, there are four low-lying occupied metal orbitals and one high-lying virtual metal orbital. Bursten and Cayton found a similar electronic relationship to exist between specific high-valent and low-valent piano-stool complexes.<sup>9</sup> In the case of the  $d^0$ - $d^{10}$  structural relationship, an orbital scheme can be constructed in a manner directly analogous to that used in the derivation of the  $d^2$ - $d^8$  relationship.

#### Appendix

Molecular orbital calculations were performed at the Indiana University Computational Chemistry Center using a VAX 11/780 computer system, and the Fenske-Hall approximate MO method.<sup>10</sup> The atomic parameters of the model complexes,  $\text{Mo}(\text{OH})_4$  and  $\text{Mo}(\text{OH})_4^{2+}$ , were generated assuming the following bond lengths:  $\text{Mo-O} = 1.68 \text{ \AA}$ ,  $\text{O-H} = 0.957 \text{ \AA}$ . The geometries of the intermediates in the  $T_d \rightleftharpoons D_{4h}$  transformation are specified in the text.

All atomic wave functions were generated by using the method of Bursten, Jensen, and Fenske.<sup>11</sup> Contracted double- $\zeta$  representation were used for the Mo 4d and the O 2p AO's. An exponent of 1.16 was used for the H 1s AO.<sup>12</sup> The basis function for Mo was derived for the +2 oxidation state with the 5s and 5p exponents fixed at 1.80. The calculations were performed by using a fragment approach. The  $(\text{OH})_4^{4-}$  ligand set was converged separately; the resulting *molecular* orbitals were then allowed to interact with the metal center. All calculations were converged with a self-consistent field iterative technique by using a convergence criteria of 0.0010 as the largest deviation between atomic orbital populations for successive cycles. In the "frozen  $\pi$ -orbital" method, the ligand  $\pi$  orbitals of the  $(\text{OH})_4^{4-}$  canonical basis are partitioned in the Fock and overlap matrices in a similar fashion to the partitioning of the matrices of a diatomic molecule into core and valence regions as illustrated by Roothaan.<sup>7</sup> The  $\pi$  orbitals are then deleted from variational treatment.<sup>13</sup>

**Acknowledgment.** We thank the National Science Foundation for support. R.H.C. is a 1988 Chester Davis Fellow and a 1989 National Science Foundation Postdoctoral fellow.

(9) Bursten, B. E.; Cayton, R. H. *Organometallics* **1987**, *6*, 2004.

(10) Hall, M. B.; Fenske, R. F. *Inorg. Chem.* **1972**, *11*, 768.

(11) Bursten, B. E.; Jensen, J. R.; Fenske, R. F. *J. Chem. Phys.* **1978**, *68*, 3320.

(12) Hehre, W. J.; Steward, R. F.; Pople, J. A. *J. Chem. Phys.* **1969**, *51*, 2657.

(13) An excellent discussion and details of the computational procedure have been presented: Lichtenberg, D. L.; Fenske, R. F. *J. Chem. Phys.* **1976**, *64*, 4247.